Real-time pulse oximetry extraction using a lightweight algorithm and a task pipeline scheme

John Vourvoulakis
Dpt. of Computer, Informatics and Telecommunications Engineering
International Hellenic University
Serres, Greece
jvourv@ihu.gr

Leonardos Bilalis
Dpt. of Industrial Management and Technology
University of Piraeus
Piraeus, Greece
leonardob@unipi.gr

***Abstract*—Pulse oximetry is a popular non-invasive method for monitoring the oxygen saturation levels (SpO_2) in blood as well as the heart rate (HR) of a patient. The photoplethysmographic signal (PPG) is used to estimate SpO_2 and HR. It indicates the light absorption of oxygenated and deoxygenated hemoglobin at a certain wavelength. Red and IR wavelengths are often used to extract PPG signals. Subsequently, various algorithms can be applied to the PPG signals in order to obtain SpO_2 and HR. In this paper, we propose a pulse oximetry system in which a lightweight algorithm is applied for HR and SpO_2 estimation. Our study was based on PPG signals derived from the MAX30102 sensor. PIC18F46Q43 microcontroller unit (MCU) was selected as the system processor, which was responsible for the sensor readouts and for the implementation of the algorithm. Communication with each external device was accomplished by using Direct Memory Access (DMA) transfers. Furthermore, the required functionality was deployed by adopting a task pipeline firmware scheme. In that scheme, operations were completed in parallel. This technique accelerated the execution and maximized the time in which the MCU can be put in low power mode. Interconnection between our system and a personal computer was also realized by using an external USB-to-serial module. Associated Octave scripts for receiving, analyzing and processing of PPG signal data were also developed.**

Keywords*—*real-time, pulse oximetry, photoplethysmogram (PPG), SpO_2, heart rate (HR), task pipeline

I INTRODUCTION

Oxygen saturation in blood (SpO_2) and heart rate (HR) constitute two vital signs of a patient which are closely monitored in an intensive care unit. They provide critical information about the cardiovascular system, the respiratory system, detect evidence about the presence of hypoxemia etc.

Pulse oximetry is a method for estimating SpO_2 levels as well as HR [1], [2]. SpO_2 is defined as the ratio of the oxygenated hemoglobin to the sum of oxygenated and deoxygenated hemoglobin, as in (1).

$$SpO_2 = \frac{O_2 Hb}{O_2 Hb + Hb} \tag{1}$$

The base principle of pulse oximetry depends on the pulsatile component of arterial blood and on the different light absorption from oxygenated and deoxygenated hemoglobin at various wavelengths. Two light sources, e.g. red and infrared LEDs, illuminate a thin part of a human body such as finger, earlobe, wrist etc. A photodiode is placed on the other side (referred as transmissive pulse oximetry [3] or on the same side (referred as reflective pulse oximetry [4]) of the LEDs and detects changes in light absorption at each wavelength. The produced waveform on the photodiode is called photoplethysmographic signal (PPG). Characteristics of PPG signals, such as local peaks and onsets, AC and DC components, are used to estimate oxygen saturation levels in blood.

The HR in beats per minute (BPM) is calculated by identifying the time between two consecutive peaks of a PPG signal, finding its reciprocal and finally multiplying by 60, as in (2). The estimation of SpO_2 is a bit more complex. Initially, the AC and DC components of each PPG signal are used in order to compute the ratio R, as in (3). Subsequently, the SpO_2 can be approximated by a linear equation, as in (4). Coefficients a and b are calibrated according to reference measurements.

$$HR = \frac{60}{t_{pulse}} \tag{2}$$

$$R = \frac{AC_{\mathrm{red}} / DC_{\mathrm{red}}}{AC_{\mathrm{ir}} / DC_{\mathrm{ir}}} \tag{3}$$

$$SpO_2 = a + b \cdot R \tag{4}$$

In this paper, we propose a real-time algorithm for local extrema detection of a PPG signal in order to calculate HR and SpO_2. The algorithm is lightweight and is executed in the time domain. It is based on an adaptive threshold concept which is similar to the algorithm presented in [5]. However, there are key differences rendering the proposed algorithm more reliable when high HR is detected. PPG signals are derived from a MAX30102 sensor. AC and DC components for the SpO_2 estimation are calculated based on [6]. The overall algorithm is suitable for implementation in low cost, low power, small microcontrollers. Its main aspects address power consumption issues in embedded systems powered from batteries.

PIC18F46Q43 was selected for the system implementation. Considering it is an 8-bit microcontroller, its CPU has limited processing capabilities. Nevertheless, PIC18F46Q43 is equipped with sophisticated peripherals such as DMA (Direct Memory Access) controller and flexible serial communication circuits. Each implemented operation takes advantage of those features. Communications with all peripheral devices take place using DMA transfers. Therefore, each transaction is accomplished without the intervention of the microcontroller's CPU. A task pipeline scheme is proposed in order to perform operations in parallel and minimize the required time for processing. As a result, the CPU may stay longer in sleep mode, maximizing the battery life time. The estimated SpO_2 and HR values are sent to a graphics LCD for visual verification. Furthermore, the system is able to be connected to a personal computer using the UM232H module. Octave scripts were deployed for receiving data from the pulse oximeter and for off-line processing.

Following from the above considerations, the contribution of this paper is two-fold.

- A real-time and lightweight algorithm for pulse oximetry extraction from PPG signals is proposed and implemented. The algorithm is suitable to be applied in small microcontrollers for portable and wearable devices.
- A task pipeline scheme is described for efficient microcontroller operation. In this scheme, functions are applied in parallel and transactions with external devices take place using DMA. This technique releases the CPU from the communication burden. Therefore, the time in which the microcontroller can enter sleep mode during each processing cycle is maximized, reducing power consumption.

The rest of the paper is organized as follows. In Section II, a brief literature survey is given. Section III presents the details of the implemented algorithm and the proposed system. In Section IV, experimental results are provided. Section V concludes the paper.

II Literature Survey

The related work focuses on two fields. The first one concerns algorithms for local extrema detection of PPG signals. The accurate detection constitutes the trickiest part of the PPG signal processing stages. The second one presents pulse oximeters published in the literature.

In [7], a real-time algorithm for pulse peak detection in PPG signals is proposed. Two IIR filters were applied to the PPG signals achieving to reduce the passband between 0.5 Hz and 11 Hz. Afterwards, the slope sum function (SSF) was calculated. Finally, the peak search was limited in the interval between SSF signal onsets and offsets. In [8], a nine-step algorithm for locating percussion peaks from PPG signals is presented. The authors removed baseline wandering by applying wavelet decomposition and reconstruction. Subsequent steps include differentiation, periodogram calculation, reference points extraction in order to minimize the search window. Eventually, peaks are located where the 1st differential is zero and the 2nd is negative. Reference [9] describes an algorithm for peak detection of low amplitude photoplethysmographic signals. A peak is registered when the number of consecutive samples with rising value exceeds a threshold and the first sample with falling value is met. Reference [5] presents an algorithm for real-time peak detection of photoplethysmograms. A PPG sensor and a Bluetooth module inserted into a computer mouse and the monitoring of a person's vital signs can be achieved while working. The proposed algorithm consists of two phases. In the first phase, the peaks are detected and in the second phase, false peaks are rejected. A point is considered a peak, if it constitutes a local extreme point and the distance between that point and an adjacent peak exceeds an adaptive threshold. This algorithm is quite close to the algorithm implemented in the present article, which is described in the following section.

In [3], a pulse oximeter is presented based on PIC18F4520 microcontroller. The authors used external analog circuitry for amplifying and filtering the PPG signal as well as a triggering circuit to convert it to a pulse waveform. The accuracy was compared with a commercial oximeter and was found acceptable. Reference [10] takes advantage of the arduino platform and shields to implement a patient remote monitoring system using CAN bus and Zigbee protocol. In [11], a wireless device is implemented based on a PSoC1 chip and ESP8266. PSoC1 retrieved data through UART from a commercial pulse oximeter device and ESP8266 sent data to a cloud server using MQTT protocol. In [12], a low-cost HR and SpO_2 monitor is described. The authors used the AFE4490 as Analog-Front-End and the TM4C123GH6PM as main processor. Digital filtering was applied to the PPG signal in order to remove unwanted frequencies. They used a circular buffer to store samples from 1.4 second intervals and the auto-correlation function was employed to estimate the HR. In order to calculate SpO_2, (3) was used. The least squares method was adopted to calibrate coefficients a, b. Reference values derived from a commercial pulse oximeter. In [4], a pulse oximetry device based on red and green wavelengths is presented. Analog circuitry was used for basic filtering and ESP32 module was selected to read PPG (analog) signals, apply processing and transmit results to a smart app through Bluetooth. The authors differentiated the PPG signals and checked for zero-crossing points in order to locate two consecutive peaks and a valley point between them. Only cycles producing valid HR and SpO_2 results were taken into account in the calculations. SpO_2 was approximated using a quadratic polynomial equation curve. Various length moving average windows were employed for stable results. In [13], a method for estimating HR from a PPG signal combining processing applied to both TD and FD is presented. In TD, the impulsive signal was calculated and differentiated. The zero crossing points of the produced signal were located which defined the pulse interval. In FD, the Hilbert transform was applied. The result was normalized and FFT analysis was performed. The peak FFT value represented the pulse frequency.

Using the above algorithms and implementations, the processing load for measuring oxygen levels in blood is not negligible. Some systems use 32-bit processors to meet the processing requirements, while others apply filtering functions in hardware. The proposed algorithm, presented below, combines the best aspects of existing approaches with the advanced features of a modern microcontroller in order to achieve real-time performance in a small embedded system, keeping the power consumption requirements at a minimum. In particular, it adopts the adaptive threshold concept applied in [5] for local extrema detection, which renders the required processing to a simple search in the TD. The algorithm was refined appropriately in order to increase the reliability in case of higher heart rates. Demanded computations were also reduced for estimating the AC and DC components of red and infrared waveforms by following [6]. Heavier processing tasks such as digital filtering for eliminating baseline wandering or transformations to FD were avoided, keeping the overall algorithm lighter in comparison with other approaches in the literature.

III The Proposed System

The current work was based on the sensor MAX30102. The MAX30102 constitutes a reflective pulse oximetry module. It integrates two LEDs at red and infrared wavelengths, a photodetector, noise rejection electronics, an 18-bit Analog to Digital Converter and an I^2C serial interface. The graphics LCD Nokia 5110 was selected to display HR and SpO_2 results. The LCD uses SPI communication interface. In order to send sensor data to a personal computer for off-line processing, the UM232H USB-to-serial module was used. PIC18F46Q43 was selected as the main processor which is responsible for all system operations. The block diagram of the system is depicted in Fig 1. The system can work with or without the connection to a personal computer.

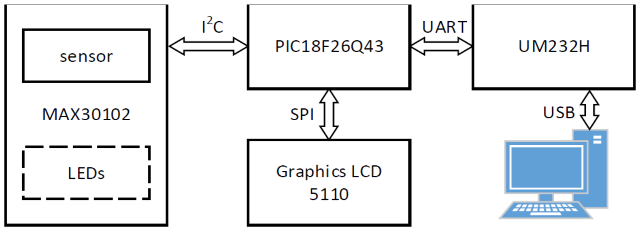

Fig.1 The block diagram of pulse oximetry system.

PIC18F46Q43 configures appropriately the MAX30102 sensor for the desired operation. ADC conversion range, LEDs pulse width and amplitude, sampling rate and FIFO buffer options are the most important operation parameters. The PPG signals for red and infrared wavelengths are read through the I^2C interface. As it has been already mentioned, peak and onset detection of the pulsatile component is required for the calculations. Post-processing usually follows for a stable output. The proposed algorithm applies first a moving average function to smooth the PPG signal. Subsequently, search in couples for peaks and onsets is conducted. A point is considered as a peak if it is the maximum along an interval that is longer than an adaptive threshold. After the point is registered as a peak, the search continues to identify an onset. A point is considered as an onset if it is the minimum along an interval that is longer than an adaptive threshold. The key difference in comparison with the approach in [5] is that the search for peaks and onsets occurs simultaneously, although local extrema are registered alternately. When a new sample arrives, it is compared with both temporary local extrema no matter if it is turn to register a peak or an onset. However, the sample will be registered as a peak or an onset only if it satisfies the threshold criterion at a subsequent time. The reason behind that is because a local minimum can be met before a local maximum is registered and the opposite. In [5], the search is conducted first to locate a peak. When a peak is registered, then the search is conducted to find an onset. The proposed modification in the current paper improved the peak detection when the HR is more than 130 bpm. The algorithm for peaks and onsets detection is quoted in Table I.

TABLE I. THE PROPOSED ALGORITHM

Step	Action
1.	Read PPG sample
2.	Apply moving average

3.	Search for local maxima
	if (PPG_sample > max)
	    max = PPG sample
	    $time_{max}$ = current_timeslot

4.	Search for local minima
	if (PPG_sample < min)
	    min = PPG sample
	    $time_{min}$ = current_timeslot

5.	Check if current time exceeds threshold
	if ((current_timeslot - $time_{max}$) > threshold
	    && last_extrema_was_min == true)
	    Register max as local maximum
	    Calculate HR

6.	Check if current time exceeds threshold
	if ((current_timeslot - $time_{min}$) > threshold
	    && last_extrema_was_max == true)
	    Register min as local minimum
	    Calculate ACred, DCred, ACir, DCir, R
	    Calculate SpO_2

7.	Compute mean value from the last 8 estimations
8.	Select new threshold from LUT based on HR

A second difference is that the threshold is updated from a LUT (Look-Up-Table) and it is optimized for the proposed system. The threshold value depends on the HR. In general, higher HR values imply lower threshold values. In order to determine the thresholds in detail, we produced some datasets using the proposed system and processed them off-line. Each threshold was selected only if achieved to locate all peaks and onsets in the specified HR range according to our datasets. The threshold for HR higher than 160 bpm was estimated arbitrarily. The LUT for the adaptive threshold assignment is presented in Table II.

TABLE II. LUT FOR THE ADAPTIVE THRESHOLD.

HR (in BPM)	Threshold (in ms)
160 < HR	180
140 ≤ HR < 160	200
120 ≤ HR < 140	220
100 ≤ HR < 120	250
80 ≤ HR < 100	280
70 ≤ HR < 80	320
60 ≤ HR < 70	360
HR < 60	400

After locating local extrema, the calculations for HR and SpO_2 levels apply as follows. In Fig. 2, let us consider A_{pre}, A_{cur} two successive peaks and B_{pre}, B_{cur} two successive onsets. The HR is calculated as in (2), where $t_{pulse} = t_{max\_cur} - t_{max\_pre}$. The SpO_2 level is estimated based on [6]. Consider as L the line passing through the onset points A_{pre} and A_{cur}. Let us set as C the point of the line at $t = t_{max\_cur}$. The AC component of the PPG signal is approximated by the distance between points B_{cur} and C. The DC component of the PPG signal is approximated as c_y. The equation of line L (5) is determined as in (6) and (7).

$$y(t) = d \cdot t + f \tag{5}$$

$$d = \frac{PPG_{min\_cur} - PPG_{min\_pre}}{t_{min\_cur} - t_{min\_pre}} \tag{6}$$

$$f = PPG_{min\_cur} - d \cdot t_{min\_cur} \tag{7}$$

The DC component of the PPG signal is calculated as in (8). The AC component of the PPG signal is estimated by subtracting the DC component from the PPG_{max_cur} value.

$$DC = d \cdot t_{max\_cur} + f \tag{8}$$

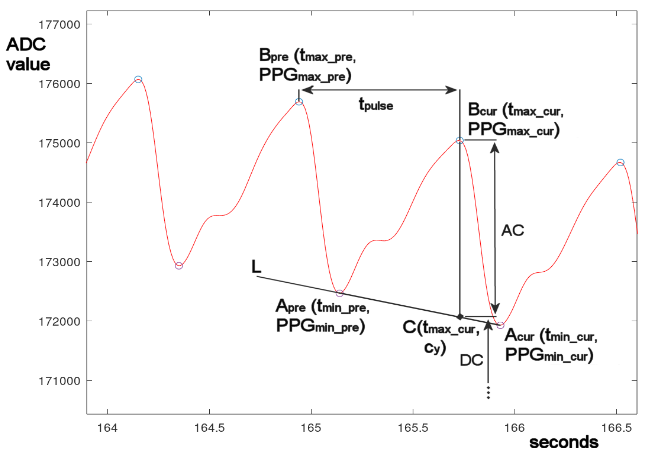

Fig.2 HR and SpO_2 calculations.

The same calculations hold for both red and infrared PPG signals. Since the AC and DC components are available for red and infrared wavelengths, ratio R is calculated as in (3) and the SpO_2 level in blood is estimated as in (4). Calibration values are provided by [6], where a = 104 and b = –17.

Fig. 2 was constructed assuming a sampling rate of 100 samples/sec. This means that each new sample arrives every 10 ms. The waveform is depicted for an interval about 1.6 seconds and it includes about 160 samples. The MAX30102 includes a FIFO buffer of 32 bytes for storing PPG signals. Each sample occupies 3 bytes. Therefore, 30 bytes are required to save 5 samples of red and infrared waveforms. Moreover, the MAX30102 is configured to assert an interrupt when 30 unread bytes (5 samples of each red and infrared PPG signals) have been stored in its FIFO buffer. Taking into account the sampling rate, which is configured at 100 samples/sec, this means that the interrupt request signal asserts every 50 ms. The microcontroller's tasks include the readout from the sensor, the processing of raw data, the transmission of raw data to a personal computer and the transmission of the results to the LCD. When all operations are required, these tasks should be performed in each interrupt request. The transmission of the results to the LCD could be limited to one transfer every a few seconds since the screen contents update is not critical for monitoring purposes. Nevertheless, we include the transmissions to the LCD in the pipeline since it gives a better picture of the proposed system's design concept.

In order to accelerate execution of all system operations, PIC18F46Q43 applies a task pipeline scheme using DMA transfers for communication with all peripherals. This scheme achieves parallelism of operations. In the first interrupt, at time t_0, the MCU acquires data from the MAX30102 through the I^2C interface. Data points are stored in the microcontroller's RAM and no other activity is performed. The second interrupt will take place after 50 ms. Let us set this time slot as t_1. The MCU reads data at time t_1 through I^2C using DMA transfers. At the same time, the MCU sends raw data from the previous acquisition (at t_0) to its UART and processes them accordingly. The operations do not interfere with each other and take place concurrently since the I^2C and UART transactions are performed without the CPU intervention. In the third interrupt, the MCU reads data at time t_2. The MCU sends to UART and processes data which concern time t_1. Furthermore, it transmits to the LCD the results produced from data read at time t_0. This task pipeline scheme continues perpetually. The required time for the I^2C transactions is about 2.4ms. The processing time depends on the if conditions of the implemented algorithm, however, it is not longer than 1ms for the worst case. As worst case is considered the time in which an onset is registered and the SpO_2 computations take place. About 3.3ms are required for UART transmission and 0.8ms for SPI transfers. The scheme is depicted in Fig. 3. The overall time in which the microcontroller is required to be in operating mode equals to the longest lasting operation. If a polling or interrupt based scheme had been applied, the required time would have been significantly higher. In particular, the microcontroller can be placed in low power mode for about 46 ms out of a cycle of 50 ms. CPU and peripherals are required in operation for less than 3.3ms. In addition to that time, a small time interval is taken into consideration which concerns the high frequency internal oscillator (HFINTOSC) wake-up from sleep start-up time. The microcontroller's power consumption was significantly reduced by using this scheme and was measured less than 3mW.

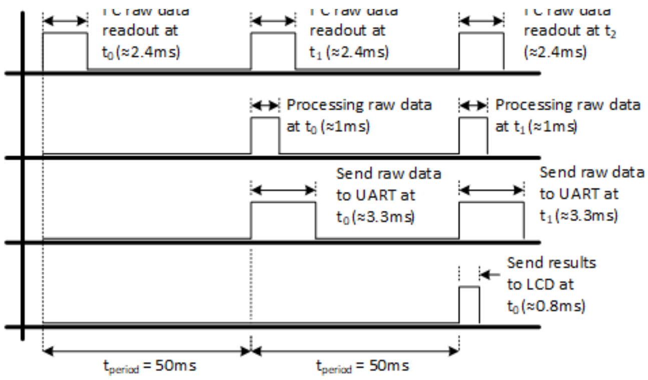

Fig.3 The task pipeline scheme.

The firmware for the microcontroller was implemented in bare metal using the MPLAB X IDE and the XC8 compiler. Fixed point arithmetic was used to accelerate the processing stage since floating point operations are time consuming. Furthermore, Octave scripts were developed for receiving raw data and for off-line processing.

IV EXPERIMENTAL RESULTS

In pulse oximetry, the subtle point is the accurate detection of peaks and onsets. The adaptive threshold is necessary in order for the system to be able to perform reliably at low and high HR. In Fig. 4, results for extrema detection are presented for HR at rest. In Fig. 5, results are provided after intense activity. Peaks and onsets have been successfully detected in both cases.

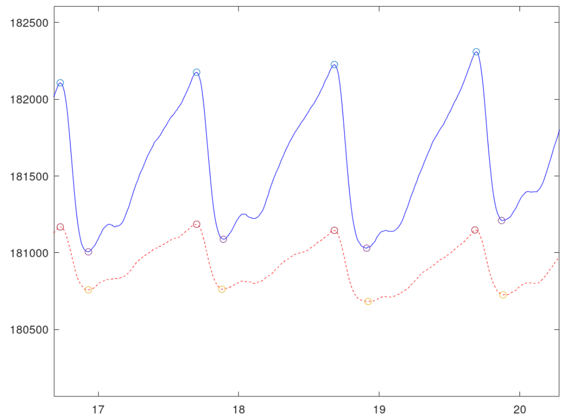

Fig.4 Peak and onset detection. Solid line: infrared, dashed-line: red. Estimated values: HR=61bpm, SpO_2=97%.

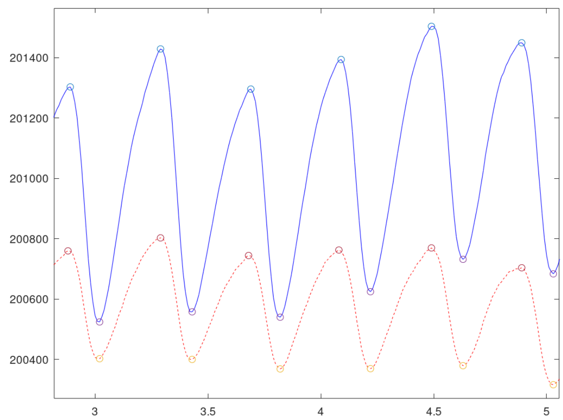

Fig.5 Peak and onset detection. Solid line: infrared, dashed-line: red. Estimated values: HR=150bpm, SpO_2=96%.

In order to evaluate the accuracy and to test the overall system's operation, we compared the results from the proposed system with the results from a commercial pulse oximeter. A human subject underwent to a physical activity for a short time period until the pulse rate reached about 120-130 bpm. Subsequently, the subject stopped exercising and started resting. While resting, oximetry indications were recorded from both oximeters until the pulse rate fall under 70 bpm. The recording took about 3 minutes and the measurements are presented in Table III. The results show that the proposed system has similar indications with the commercial oximeter.

TABLE III. COMPARISON WITH COMMERCIAL PULSE OXIMETER.

Time (sec)	**Proposed System**		**Commercial Oximeter**	
	HR (bpm)	***SpO_2 (%)***	***HR (bpm)***	***SpO_2 (%)***
10	124	98	126	98
20	120	98	121	98
30	117	98	117	98
40	107	97	109	97
50	99	98	101	97
60	91	98	93	97
70	83	98	86	97
80	81	99	82	97
90	78	98	80	97
100	76	98	78	97
110	74	98	76	97
120	72	98	74	97
130	71	98	72	97
140	71	98	70	96
150	69	98	68	96
160	67	97	67	96

In Fig. 6, a photo of the system in operation is presented, along with the commercial pulse oximeter. The proposed system is attached to the index finger, while the commercial oximeter is attached to the middle finger of the same human subject. The microcontroller PIC18F46Q43-I/P is located in the center of the photo, while the MAX30102 sensor is located under the forefinger.

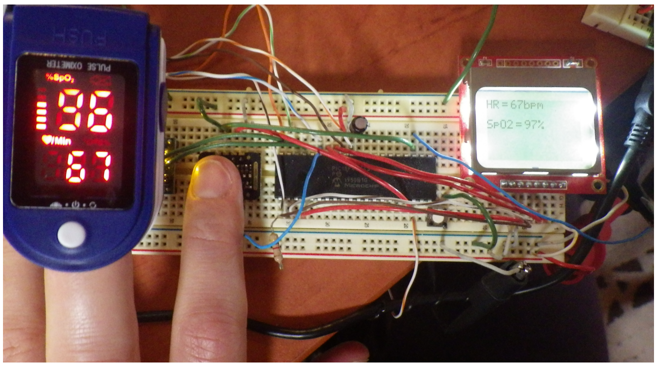

Fig.6 A photo of the test rig in operation.

V CONCLUSION

In this paper, a pulse oximetry system was implemented. In order to calculate HR and SpO_2 levels in blood, a lightweight algorithm was applied in the time domain for peak and onset detection, as well as for AC and DC components of PPG signals. A task pipeline technique was adopted for the system operation, which in conjunction with DMA transfers achieved to optimize the system performance. The system operated with significantly low power requirements providing comparable results with commercial pulse oximeters. Future work consists of a comprehensive study of algorithms and experiments for motion artifact removal.

REFERENCES

1 A. Jubran, “Pulse oximetry,” *Crit. Care*, vol. 3, no. 2, 1999.

2 A. Jubran, “Pulse oximetry,” *Crit. Care*, vol. 19, no. 1, 2015.

3 A. Y. H. Elagha, A. A. H. El-Farra, and M. H. K. H. Shehada, “Design a non-invasive pulse oximeter device based on PIC microcontroller,” in *Proceedings - 2019 International Conference on Promising Electronic Technologies, ICPET 2019*, 2019, pp. 107–112.

4 P. P. Banik, S. Hossain, T.-H. Kwon, H. Kim, and K.-D. Kim, “Development of a wearable reflection-type pulse oximeter system to acquire clean ppg signals and measure pulse rate and spo<inf>2</inf> with and without finger motion,” *Electron.*, vol. 9, no. 11, pp. 1–26, 2020.

5 T. V. Tran and W.-Y. Chung, “A Robust Algorithm for Real-Time Peak Detection of Photoplethysmograms Using a Personal Computer Mouse,” *IEEE Sens. J.*, vol. 15, no. 8, pp. 4651–4659, 2015.

6 M. Smith, “Recommended Configurations and Operating Profiles for MAX30101/MAX30102 EV Kits,” Maxim Integrated Products, Application Note: 6409, 2018.

7 D.-G. Jang, S. Park, M. Hahn, and S. Park, “A Real-Time Pulse Peak Detection Algorithm for the Photoplethysmogram,” *Int. J. Electron. Electr. Eng.*, pp. 45–49, 2014.

8 F. Luo, J. Li, F. Yun, T. Chen, and X. Chen, “An improved algorithm for the detection of photoplethysmographic percussion peaks,” in *Proceedings - 2014 7th International Congress on Image and Signal Processing, CISP 2014*, 2014, pp. 902–906.

9 E. J. A. Prada, “The mountaineer's method for peak detection in photoplethysmographic signals | El método del alpinista para detección de picos en señales fotopletismográficas,” *Rev. Fac. Ing.*, vol. 2018, no. 90, 2018.

10 L. C. Banuag and J. K. G. Salva, “Development of a Patient Monitoring System for Hospital Wards Employing Zigbee Technology and CAN Protocol,” in *Proceedings of 2019 2nd World Symposium on Communication Engineering, WSCE 2019*, 2019, pp. 112–116.

11 T. J. Jeyaprabha, A. Abijith, G. Prashanth, and T. Chiranjeevraja, “Implementation of remote patient monitoring using wireless pulse oximeter,” *Int. J. Recent Technol. Eng.*, vol. 7, no. 5, pp. 458–463, 2019.

12 A. T. Ayance, H. S. Ramirez, J. M. R. Perez, and C. G. T. Palacios, “Low-cost microcontrolled based wireless heart rate and oxygen saturation monitor,” in *2018 28th International Conference on Electronics, Communications and Computers, CONIELECOMP 2018*, 2018, vol. 2018-Janua, pp. 176–180.

13 P. M. Mohan, V. Nagarajan, and J. C. Vignesh, “Spot and continuous monitoring of heart rate by combining time and frequency domain analysis of photoplethysmographic signals at rest conditions,” *IET Signal Process.*, vol. 11, no. 9, pp. 1076–1082, 2017.